LBNL-40196
UC-1501

ERNEST ORLANDO LAWRENCE
BERKELEY NATIONAL LABORATORY

On the Differences in the Reaction Mechanism for CO and CO/H_2 Electrooxidation on PtRu and PtSn Alloy Electrodes

H.A. Gasteiger, N.M. Marković, and P.N. Ross, Jr.
Materials Sciences Division

April 1997

REFERENCE COPY
Does Not
Circulate
Bldg. 50 Library - Ref.
Lawrence Berkeley National Laboratory
Copy 1
LBNL-40196

DISCLAIMER

This document was prepared as an account of work sponsored by the United States Government. While this document is believed to contain correct information, neither the United States Government nor any agency thereof, nor The Regents of the University of California, nor any of their employees, makes any warranty, express or implied, or assumes any legal responsibility for the accuracy, completeness, or usefulness of any information, apparatus, product, or process disclosed, or represents that its use would not infringe privately owned rights. Reference herein to any specific commercial product, process, or service by its trade name, trademark, manufacturer, or otherwise, does not necessarily constitute or imply its endorsement, recommendation, or favoring by the United States Government or any agency thereof, or The Regents of the University of California. The views and opinions of authors expressed herein do not necessarily state or reflect those of the United States Government or any agency thereof, or The Regents of the University of California.

Available to DOE and DOE Contractors
from the Office of Scientific and Technical Information
P.O. Box 62, Oak Ridge, TN 37831
Prices available from (615) 576-8401

Available to the public from the
National Technical Information Service
U.S. Department of Commerce
5285 Port Royal Road, Springfield, VA 22161

Ernest Orlando Lawrence Berkeley National Laboratory
is an equal opportunity employer.

DISCLAIMER

This document was prepared as an account of work sponsored by the United States Government. While this document is believed to contain correct information, neither the United States Government nor any agency thereof, nor the Regents of the University of California, nor any of their employees, makes any warranty, express or implied, or assumes any legal responsibility for the accuracy, completeness, or usefulness of any information, apparatus, product, or process disclosed, or represents that its use would not infringe privately owned rights. Reference herein to any specific commercial product, process, or service by its trade name, trademark, manufacturer, or otherwise, does not necessarily constitute or imply its endorsement, recommendation, or favoring by the United States Government or any agency thereof, or the Regents of the University of California. The views and opinions of authors expressed herein do not necessarily state or reflect those of the United States Government or any agency thereof or the Regents of the University of California.

LBNL-40196
UC-1501

On the Differences in the Reaction Mechanism for CO and CO/H2 Electrooxidation on PtRu and PtSn Alloy Electrodes

H.A. Gasteiger,* N.M. Marković, and P.N. Ross, Jr.

Materials Sciences Division
Ernest Orlando Lawrence Berkeley National Laboratory
University of California
Berkeley, California 94720

April 1997

*Corresponding author:
Phone: +0049 (731) 502-5469
Fax: +0049 (731) 502-5452
e-mail: hgasteig@blitz.chemie.uni-ulm.de

This work was supported by the Assistant Secretary for Conservation and Renewable Energy, Office of Transportation Technologies, Electric and Hybrid Propulsion Division, of the U.S. Department of Energy under Contract No. DE-AC03-76SF00098.

On the Differences in the Reaction Mechanism for CO and CO/H_2 Electrooxidation on PtRu and PtSn Alloy Electrodes

H.A. Gasteiger*
Abteilung Oberflächenchemie und Katalyse, Universität Ulm
D-89069 Ulm, Germany
and
N.M. Marković and P.N. Ross (Jr.)
Lawrence Berkeley National Laboratory
Berkeley, CA 94720, USA

Summary

Electrooxidation kinetics of mixtures of carbon monoxide and hydrogen were studied on well-characterized surfaces of Pt and alloys of PtRu and PtSn in 0.5 M H_2SO_4 at room temperature and 60°C. The alloy electrode surfaces were prepared in UHV by sputter/anneal cycles and their surface compositions were determined *via* low energy ion scattering. Subsequently, the electrodes were transferred contamination-free from UHV into a rotating disk electrode (RDE) configuration in a conventional electrochemical cell and their activity was measured both by CO stripping voltammetry and under the continuous flow of CO and CO/H_2 gas mixtures in RDE-experiments.

The overpotential for the continuous oxidation of pure CO on PtSn electrodes with a Sn surface composition of $x_{Sn,s} \sim 0.2$ is significantly smaller than on PtRu alloys ($x_{Ru,s} \sim 0.5$) and on pure Pt. The reaction order with respect to solution phase CO is negative on PtRu alloys due to the competition between OH_{ads} nucleation and CO adsorption on Ru surface atoms. Owing to the lack of CO adsorption on OH_{ads}-providing Sn surface atoms, the reaction order with respect to CO is positive on PtSn electrodes. Therefore, the activity enhancement of PtSn electrodes *versus* PtRu and Pt electrodes is most pronounced in pure CO and decreases with the CO concentration in CO/N_2 and CO/H_2 mixtures.

*Corresponding author:
phone: +0049-(731)-502-5469
fax: +0049-(731)-502-5452
e-mail: hgasteig@blitz.chemie.uni-ulm.de

1. Introduction

Low-temperature polymer electrolyte membrane fuel cells (PEM-FC) are a promising alternative to internal combustion engines in vehicle applications. *State of the art* hydrogen/air PEM-FC's, operating under nearly ambient pressure at temperatures between 60 to 100°C, are capable of energy conversion efficiencies on the order of 60% at noble metal loadings as low as 0.2 mg/cm^2 /1, 2/. Because of the difficulties associated with H_2-storage in terms of weight, volume, and range of the vehicle /3/, the *on-board* production of the H_2-anode feed *via* steam reformation of methanol is envisaged /4/. The typical *reformer gas* composition from the methanol steam reformation process is ~75% H_2 in ~25% CO_2, contaminated, however, with ~1-2% CO /5/. Unfortunately, CO concentrations at this level nearly completely poison the anode catalyst (Pt, PtRu), effecting an unacceptable loss in the energy conversion efficiency of the fuel cell. Therefore, CO in the H_2-rich reformer gas must be reduced to concentrations which are compatible with the currently available anode catalysts. This, for example, can be accomplished by selectively oxidizing CO to CO_2 on oxide-supported platinum /6, 7, 8/ or on gold/transition metal oxide catalysts /9, 10/.

The CO concentration up to which the efficiency of the fuel cell with CO-contaminated H_2 is essentially identical with the efficiency achieved with pure H_2-feed, is defined by the *CO-tolerance* of the anode catalyst. For pure Pt electrodes it is on the order of 5-25 ppm, depending on the metal loading /6, 11/, while it is ~100 ppm for PtRu anode catalysts /11/. The enhanced CO-tolerance of PtRu alloy electrodes is due to their enhanced CO oxidation activity if compared to pure Pt and can be rationalized on the basis of a bifunctional mechanism in which the Ru-catalyzed nucleation of oxygen-containing species (OH_{ads}) at low electrode potentials /12/ leads to the oxidation of adsorbed CO (on either Pt or Ru sites) to CO_2 /13, 14/. Owing to the facile adsorption of CO on Ru surface atoms, the adsorption of solution phase CO is in direct competition with OH_{ads} nucleation. The ramification of this effect is a negative reaction order of the CO oxidation reaction with respect to CO partial pressure, as was demonstrated by RDE-experiments (rotating disk electrode) on well-characterized and UHV-prepared polycrystalline PtRu alloy electrodes /15/. In these RDE-experiments, where CO is being supplied continuously to the electrode surface (as is the case in the operation of a fuel cell), pure Ru is the most active surface (in the PtRu alloy system) for CO oxidation. Since, however, pure Pt is the most active H_2-oxidation catalyst, the optimized electrocatalyst for the oxidation of CO/H_2-mixtures (*i.e.*, reformer gas) at fuel cell relevant temperatures is a PtRu alloy surface with a Ru surface composition of $x_{Ru,s}$~50 atomic% /15/. Operating a PEM-FC with an anode feed of 100 ppm CO in H_2 at 80°C, a four-fold higher power density can be achieved by using a $Pt_{0.5}Ru_{0.5}$ anode catalyst instead of pure Pt /11/.

Recently, it was shown that PtSn electrodes are even more active toward the oxidation of pure CO than PtRu alloys /16, 17, 18/, a phenomenon which is paralleled by the high activity of this surface toward the gas phase oxidation of CO /19/. Similar to the bifunctional action of PtRu electrodes, the Sn-component of PtSn alloys is thought to catalyze the nucleation of OH_{ads} at low electrode potentials so that CO adsorbed on Pt surface atoms can be oxidized efficiently /17, 18/. In contrast to the PtRu system, however, gas phase studies indicate that CO does not adsorb on Sn surface atoms /20, 21/, which in turn implies that there be no competition between OH_{ads} nucleation and CO adsorption. Since this competition on PtRu surfaces was the process which lead to a negative reaction order with respect to CO partial pressure /15/, a zero or positive CO reaction order should hold for PtSn electrodes. This, indeed, has been observed for well-characterized Pt_3Sn electrodes /17, 18/.

In the present communication we will examine in detail the differences in the CO oxidation mechanism between PtRu and PtSn alloy surfaces. At first we will focus on the oxidation of pure CO, evaluating the electrode activity for the two different measurement modes, *viz.*, CO stripping voltammetry and potentiodynamic RDE-experiments at room temperature. This will highlight the fundamental difference between the two alloy systems in terms of i) the reaction order with respect to CO, ii) the CO coverage of the surface in its active state, and iii) the potential region in which the respective alloy surfaces are stable. Subsequently, we will quantify and contrast the reaction order with respect to CO for PtRu and the PtSn electrodes, employing RDE-measurements with CO/Ar mixtures at 60°C. These results are then shown to provide the basis for the understanding of the observed activity for CO/H_2 mixtures, which will be demonstrated by means of RDE-measurements with both 2 and 0.1 % CO in H_2.

2. Experimental

Most of the experimental details were described in References 14 and 17. The polycrystalline PtRu (~50 atomic% Ru) alloy and the single crystal $Pt_3Sn(110)$ alloy were prepared by sputter-anneal cycles in ultra high vacuum (UHV) with a final low-energy sputtering step (0.5 keV Ar^+). The resulting surface composition was evaluated *via* low energy ion scattering (LEIS), yielding values of $x_{Ru,s}$~0.5 for the PtRu electrode and $x_{Sn,s}$~0.2 for the Pt_3Sn electrode.

All electrodes were transferred directly from UHV into the electrochemical cell and immersed under potential control at 0.05 V versus the reversible hydrogen electrode (RHE). Electrochemical experiments were then conducted <u>without</u> any prior potential cycling of the electrodes. The cleanliness of the transfer and the electrolyte, even under sustained rotation at high rotation rates, were demonstrated in our previous work /22/. For CO strip-

ping voltammetry the electrolyte (0.5 M H_2SO_4, Baker *Ultrex*) was saturated with CO with the electrode held at ~0.1 V for 3 min. and then purged with Ar prior to recording the stripping voltammogram. For RDE-experiments, the electrolyte was equilibrated for 5 minutes with the respective gas (mixture) while the electrode potential was maintained at 0.05 V. Subsequently, the electrodes were rotated at 2500 rpm for 3 minutes in order to allow for the complete poisoning of the electrode surface with CO (from either pure CO, CO/H_2, or CO/Ar mixtures), before potentiodynamic or potentiostatic activity data were recorded.

The pure gases as well as the CO/Ar and CO/H_2 mixtures were purchased from Matheson (Matheson purity: 4N CO, 5N5 Ar, 6N H_2). Compositions of the gas mixtures were 0.1% CO/H_2, 2% CO/H, 2% CO/Ar, and 26% CO/Ar. All potentials in this work are referred to the RHE reference scale and current densities are based on the geometric surface area (0.283 cm^2) of the rotating disk electrodes prepared in UHV for which the surface roughness factor is one.

3. Results and Discussion

3.1. CO Stripping *versus* CO-RDE at Room Temperature

A comparison of the well-known CO stripping voltammetry on UHV-prepared Pt and PtRu surfaces ($x_{Ru,s}$~0.5) at room temperature (Fig. 1) clearly shows the significantly higher activity of the alloy surface toward the oxidation of adsorbed CO. Based on the stripping peak potential, the overpotential for CO oxidation on the PtRu electrode is approximately 0.25 V lower than on pure Pt /13/. Essentially the same catalytic shift between Pt and PtRu electrodes can be observed for the continuous oxidation of CO in an RDE-experiment with CO saturated electrolyte (dashed lines in Fig. 1), with the striking difference that the onset of CO oxidation is shifted toward higher electrode potentials by roughly 0.2 V. This phenomenon has already been discussed previously /15/ and is due to the negative reaction order with respect to solution phase CO and holds for all Ru surface compositions in the PtRu alloy system.

A very different behavior can be observed for PtSn electrodes. In the potential range in which PtSn alloys are stable (up to ~0.6 V at room temperature), preadsorbed CO cannot be completely stripped and the surface remains blocked to a large extent with adsorbed CO. The small stripping peak during the first positive-going sweep (solid line in Fig. 2a) resembles the pre-wave reported for both polycrystalline Pt /23/ and carbon supported high-surface area PtSn electrodes /24, 25/. The voltammetric charge under the pre-wave on the PtSn electrode is ~90 $\mu C/cm^2$ and is only a small fraction of the total CO stripping charge

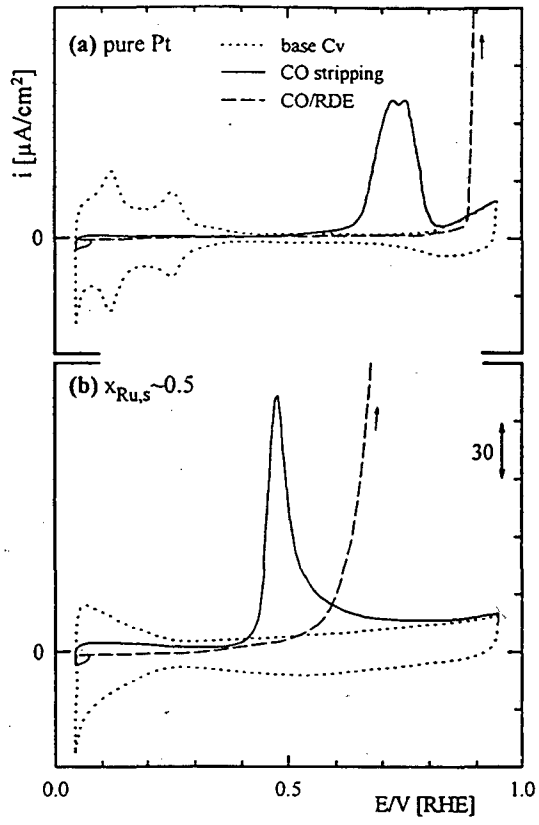

Fig. 1. Base voltammogram (· · · · · ·), CO stripping voltammogram (———), and continuous CO oxidation in a RDE configuration at 1600 rpm (— — —): **(a)** polycrystalline Pt-disk electrode; **(b)** UHV-prepared (sputtered with 0.5 keV Ar^+) PtRu(polycryst.) electrode with $x_{Ru,s}$~0.5. Experiments were conducted at room temperature in 0.5 M H_2SO_4 at sweep rate of 20 mV/s.

of either ~380 μC/cm^2 for polycrystalline Pt (Fig. 2c) or ~350 μC/cm^2 for Pt(110) /26/. The coulmetric charge in the hydrogen region (0.05 to 0.40 V) after pre-wave stripping is ~35 μC/cm^2 in contrast to ~125 μC/cm^2 for the clean UHV-prepared $Pt_3Sn(110)$ surface (dotted line in Fig. 2a). This difference of ~90 μC/cm^2 (assuming that the oxidation of CO requires 2 electrons per site) implies that a CO coverage equivalent to ~180 μC/cm^2, *i.e.*, roughly two thirds of the initially adsorbed amount of CO, remains on the $Pt_3Sn(110)$ surface if it is cycled within the stable potential range (up to 0.55 V as in Figure 2a). The total adsorption charge for CO then corresponds to ~270 μC/cm^2 and is consistent with the above values for a Pt(110) electrode if it is taken into account that ~20% of the Pt surface atoms are substituted by Sn atoms ($x_{Sn,s}$~0.2) which do not provide CO adsorption sites. Therefore, the $Pt_3Sn(110)$ surface remains largely poisoned with adsorbed CO in the potential range up to 0.55 V. Complete stripping of adsorbed CO can only be achieved at significantly higher electrode potentials (Fig. 2b) concomitant with tin dissolution. The latter is apparent from the fact that the voltammogram following the stripping experiment to high electrode potentials (dotted line in Fig. 2b) is essentially identical with the voltammetric signature of a Pt(110) electrode in sulfuric acid. The total charge for CO stripping

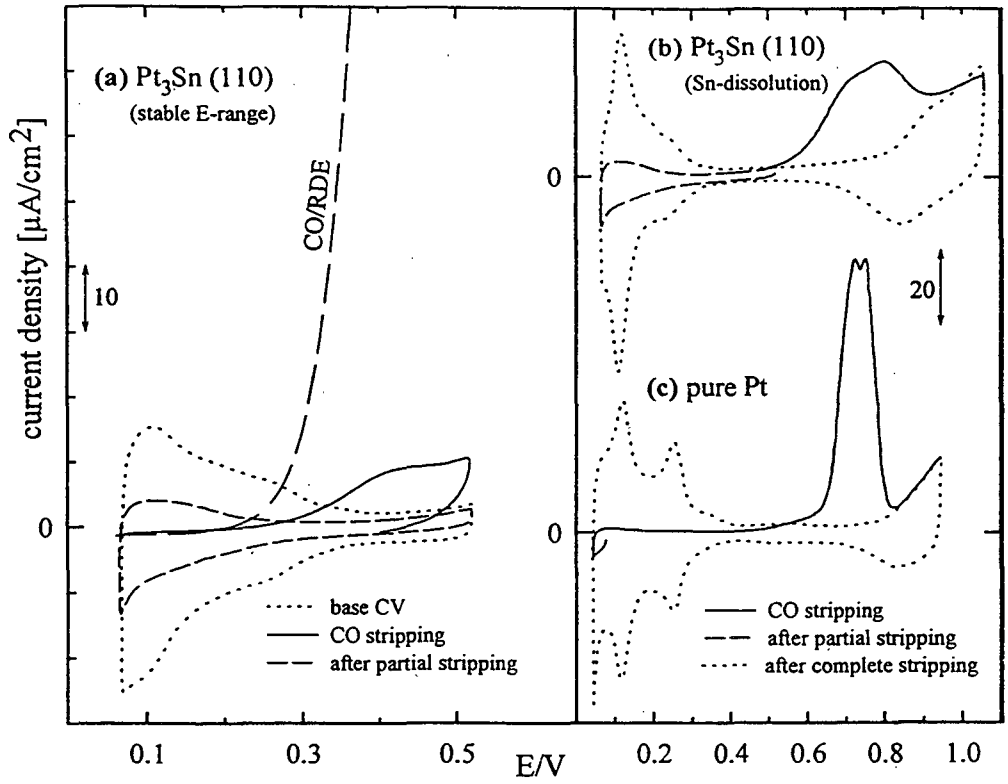

Fig. 2. **(a)** Base voltammogram (· · · · · ·), CO stripping voltammogram (———), and continuous CO oxidation in a RDE configuration at 1600 rpm (— — —) of a UHV-prepared (sputtered with 0.5 keV Ar^+) $Pt_3Sn(110)$ electrode with $x_{Sn,s} \sim 0.2$. **(b)** Same electrode as in (a) but with a positive potential limit beyond the stability region of the Pt_3Sn-alloy. **(c)** Polycrystalline Pt-disk for comparison. Experiments were conducted at room temperature in 0.5 M H_2SO_4 at sweep rate of 20 mV/s.

and tin dissolution in Figure 2b amounts to ~280 μC/cm^2. On the basis of the above estimate, this overall stripping charge should contain a contribution of ~180 μC/cm^2 from true CO oxidation and ~100 μC/cm^2 from the dissolution of Sn (as Sn^{4+}). A comparison of the CO stripping behavior on the $Pt_3Sn(110)$ surface (Fig. 2b) with UHV-prepared polycrystalline Pt (Fig. 2c) shows a close correspondence between the potential regions in which CO is being stripped from both surfaces, implying that a large fraction of the adsorbed CO is "Pt-like" and not influenced by the presence of Sn.

Although the $Pt_3Sn(110)$ surface is largely poisoned with adsorbed CO at potentials below 0.55 V, its activity for the continuous oxidation of CO in an RDE-experiment in CO saturated electrolyte is surprisingly high (long dashed line in Fig. 2a). At room temperature, potentiodynamic (20 mV/s) CO oxidation currents of 100 μA/cm^2 are attained at already ~0.38 V, approximately 0.3 V lower than on the PtRu alloy ($x_{Ru,s}$~0.5, Fig. 1b) and 0.45 V lower than on a polycrystalline Pt electrode (Fig. 1a) /27/ (it should be noted, that mass transport resistances at 1600 rpm are negligible for this current density). On the basis of the CO stripping behavior, the extremely high activity of the sputtered $Pt_3Sn(110)$ surface for the oxidation of solution phase CO can only be rationalized under the assumption of a negative reaction order with respect to CO, a point to which we will return in Section 3.3.

3.2. CO Stripping *versus* CO-RDE at 60°C

At 60°C, the difference in activity between the oxidation of adsorbed CO (stripping voltammetry, 20 mV/s) and solution phase CO (RDE, 1 mV/s) for PtSn electrodes on one hand and PtRu and Pt electrodes on the other hand follows the trends which were observed at room temperature: on PtRu (Fig. 3a) and Pt (Fig. 3c), the activity toward the oxidation of preadsorbed CO is higher than toward solution phase CO; on PtSn (Figs. 3b and 3c), solution phase CO is oxidized long before the complete oxidation of preadsorbed CO. As before, the continuous oxidation of solution phase CO on the PtSn electrode proceeds on a largely CO covered surface (the pre-wave desorption is not shown in Fig. 3a) and complete CO stripping occurs at similar electrode potentials as on pure Pt (Fig. 3c and 3d) with a concomitant loss of Sn from the alloy surface.

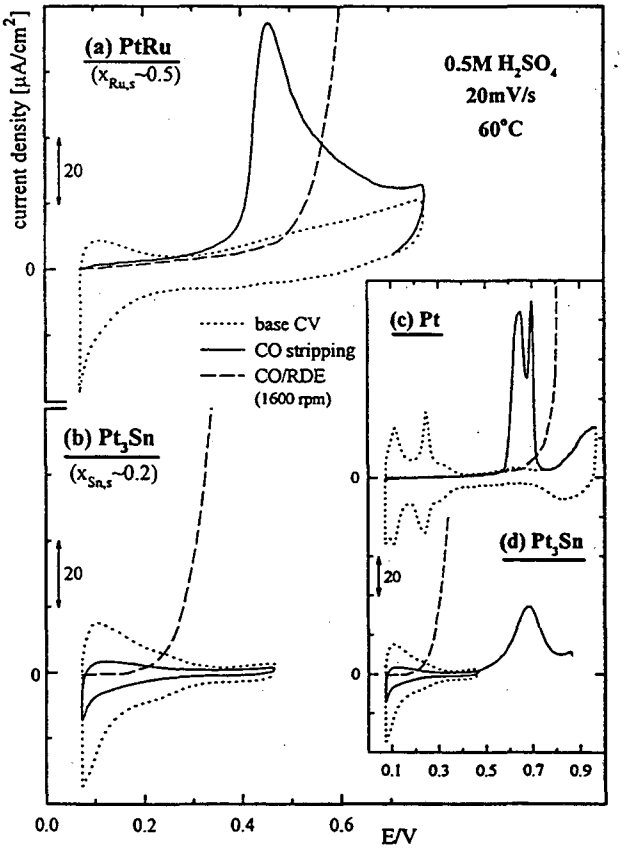

Fig. 3. Base voltammogram (· · · · · ·), CO stripping voltammogram (———), and continuous CO oxidation in a RDE configuration at 1600 rpm (— — —): **(a)** of a UHV-prepared (sputtered with 0.5 keV Ar^+) PtRu(polycryst.) electrode with $x_{Ru,s}$~0.5; **(b)** of a UHV-prepared (sputtered with 0.5 keV Ar^+) $Pt_3Sn(110)$ electrode with $x_{Sn,s}$~0.2. Comparison of the complete CO stripping: **(c)** on polycrystalline Pt; **(d)** on the Pt_3Sn-surface of (b). Experiments were conducted at 60°C in 0.5 M H_2SO_4 at 20 mV/s.

3.3. Reaction Order with Respect to CO at 60°C

At both 25° and 60°C, the comparison between CO stripping voltammetry and CO-RDE activity points toward a negative reaction order with respect to solution phase CO on the Pt and PtRu surfaces and a positive reaction order for PtSn surfaces. RDE experiments with various mixtures of CO in Argon and pure CO allow for a quantitative evaluation of the reaction order at a given electrode potential. Figure 4a shows a set of measurements at 60°C on the sputtered $Pt_3Sn(110)$ electrode surface, with a magnification of the low current density region displayed in the inset (Fig. 4b). It is apparent that the quasi-steady-state (1 mV/s) CO oxidation activity of the PtSn alloy electrode increases with the partial pressure of CO in the gas mixture, contrary to what is observed for Pt and PtRu electrodes /15/.

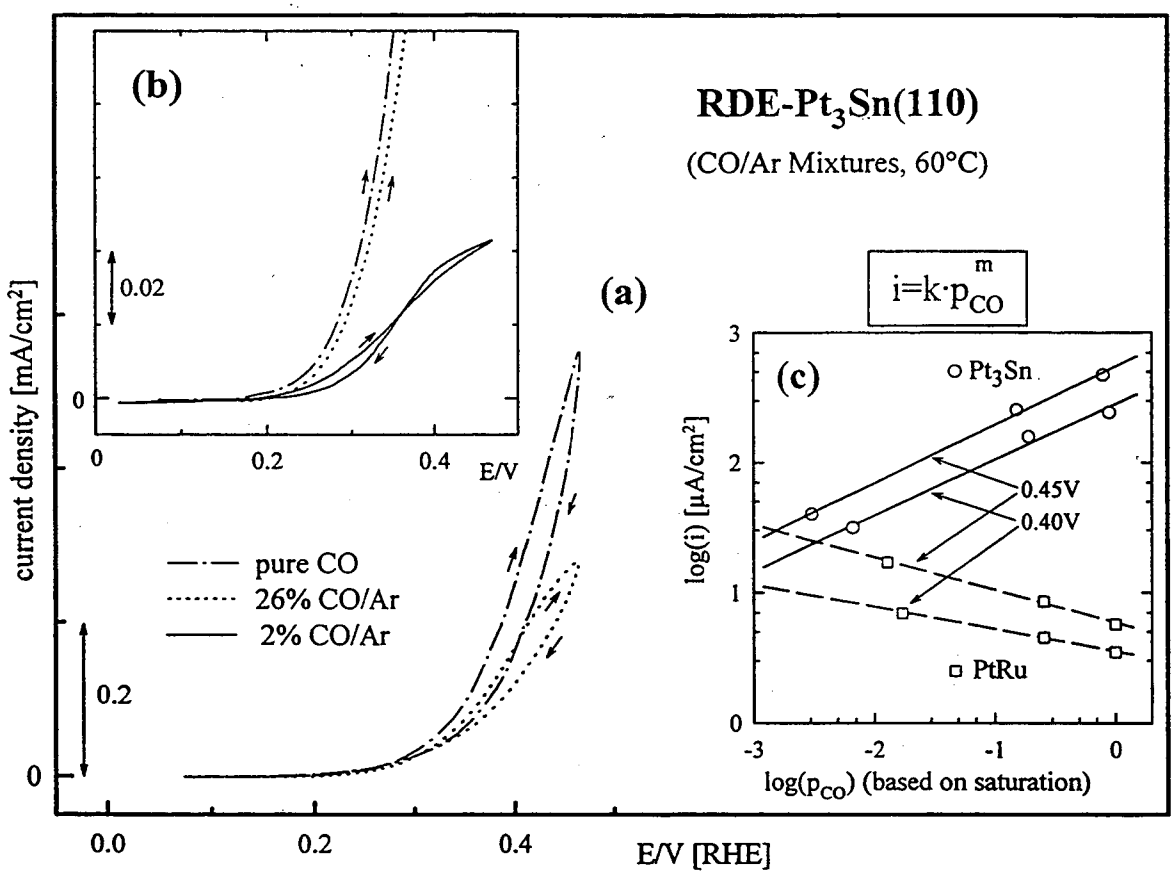

Fig. 4. **(a)** Potentiodynamic (1 mV/s) oxidation current densities for pure CO and CO/Ar mixtures on a UHV-prepared (sputtered with 0.5 keV Ar^+) $Pt_3Sn(110)$ electrode with $x_{Sn,s} \sim 0.2$ at 2500 rpm in 0.5 M H_2SO_4 at 60°C. **(b)** Magnification of the low-current-density region using the positive-going sweeps for pure CO and 26% CO/Ar and the complete voltammogram for 2% CO/Ar. **(c)** Reaction order plot at 0.40 and 0.45 V for the Pt3Sn electrode of (a) and for the PtRu electrode of Fig. 3a (the CO concentration in the solution phase at the electrode surface is calculated from the limiting current density for each CO/Ar mixture: 2330, 630, and 47 $\mu A/cm^2$ at 100% CO, 26% CO/Ar, and 2% CO/Ar, respectively). Before each measurement, the potential was held at ~0.05 V for 3 min. at a rotation rate of 2500 rpm.

Since the diffusion limited current density of CO can be determined experimentally /15/, the CO concentration at the electrode/electrolyte interface (relative to saturation with pure CO) can be calculated *via* the mass transfer properties of the rotating disk configuration /28/. A double-logarithmic plot of current density on the $Pt_3Sn(110)$ electrode *versus* the calculated relative CO partial pressure at the electrode/electrolyte interface is shown in Figure 4c for two electrode potentials (solid lines). The slope of these two lines which is equivalent to the exponent in the power law expression shown in Figure 4 is +0.40±0.05, *i.e.*, the reaction order with respect to solution phase CO is positive for the sputtered $Pt_3Sn(110)$ electrode. The reaction order of the significantly more active well-ordered $Pt_3Sn(111)$ surface ($x_{Sn,x}$~0.25) is even more positive with a value of 0.60±0.05 /18/.

In contrast to the $Pt_3Sn(110)$ surface, the reaction order with respect to solution phase CO on the PtRu electrode at the same electrode potential is negative, namely -0.20±0.05. This behavior is expected for a Langmuir-Hinshelwood mechanism, where the adsorption sites for oxygen nucleation (Ru surface atoms) are being blocked by the adsorption of CO and is consistent with the idea of a competition between OH_{ads} nucleation and CO adsorption on Ru surface atoms /15/:

$$M-CO + Ru-OH_{ads} \longrightarrow CO_2 + H^+ + e^- + M + Ru \qquad \text{with M being either Pt or Ru}$$

Upon the onset of CO oxidation during a CO-RDE experiment with either pure CO or CO/Ar mixtures, the CO concentration at the electrode/electrolyte interface decreases continuously as the CO oxidation current increases because of the formation of a CO concentration gradient in the mass transfer boundary layer. For electrode kinetics with a negative reaction order with respect to solution phase CO this implies, that the CO oxidation activity increases with both the electrode potential and the CO oxidation current since the latter effectively reduces the CO concentration at the electrode/electrolyte interface. Therefore, for Pt and PtRu electrodes, the transition from almost zero CO oxidation currents to the diffusion limited current density occurs in a very narrow potential range, as is shown in Figure 5a for the oxidation of 2% CO in Ar (dashed and dotted lines). It is in many ways similar to the observed *ignition temperature* for the gas phase oxidation of CO and CO/H_2 mixtures on supported Pt catalysts /29, 8/, so that one might refer to the electrochemical analogue as an *ignition potential.*

On the other hand, for electrode kinetics with a positive reaction order with respect to solution phase CO (*e.g.*, the PtSn surface), the decrease of the CO concentration at the electrode/electrolyte interface with increasing CO oxidation currents produces a decrease in the CO oxidation activity. Consequently, the transition from low current densities to the diffusion-limited current density occurs gradually (Fig. 5a), in sharp contrast to the fairly well-defined *ignition potential* for Pt and PtRu electrodes. The positive reaction order on the

PtSn surface can then be rationalized if one assumes that CO does not adsorb on Sn surface atoms /20, 21/ so that the nucleation of OH_{ads} on Sn surface atoms is not hampered by the presence of solution phase CO /18/:

$$Pt-CO+Sn-OH_{ads} \longrightarrow CO_2 + H^+ + e^- + Pt + Sn$$

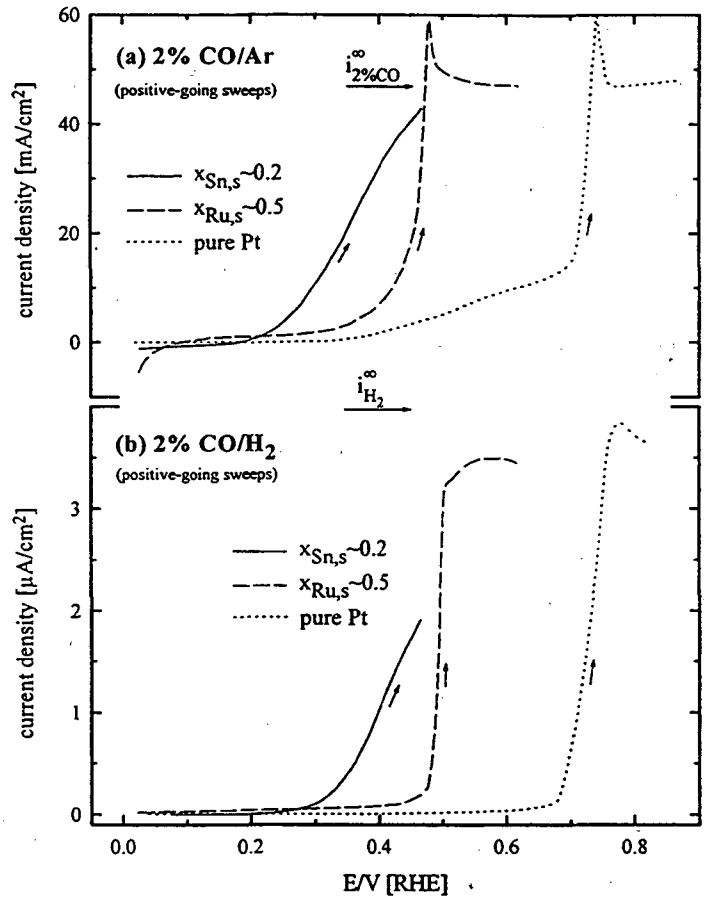

Fig. 5. Comparison of the potentiodynamic oxidation (positive-going sweeps at 1 mV/s) of (a) 2% CO/H_2 (b) and 2% CO/Ar on UHV-prepared surfaces (sputtered with 0.5 keV Ar^+): (———) $Pt_3Sn(110)$ electrode with $x_{Sn,s}$~0.2; (— — —) PtRu(polycryst.) electrode with $x_{Ru,s}$~0.5; (· · · · · ·) polycrystalline Pt-disk electrode. Experiments were conducted at 60°C in 0.5 M H_2SO_4 at 2500 rpm. The diffusion-limited current densities of CO and H_2 are marked in the Figure.

In summary, the onset of significant CO oxidation activity on Pt and PtRu surfaces is accompanied by an essentially complete stripping of adsorbed CO at the *ignition potential* (the CO stripping peak is clearly visible in Fig. 5a) and can be rationalized on the basis of the observed negative reaction order with respect to solution phase CO. In the case of PtSn alloys, the CO oxidation activity increases gradually with the electrode potential and is first order with respect to solution phase CO. In contrast to Pt and PtRu alloys, nearly completely CO poisoned PtSn surfaces are very active for CO bulk oxidation. This high degree

of CO coverage in their active potential range is the reason for the surprisingly low activity of PtSn electrodes for the oxidation of methanol if compared to PtRu electrodes /27/.

3.4. Oxidation of CO/H_2 at 60°C

On the basis of electrode activities in a mixture of 2% CO in Ar (Fig. 5a), it is now straightforward to understand the activity of the respective electrode surfaces toward the quasi-steady-state (1 mV/s) oxidation of 2% CO in H_2 (Fig. 5b). For Pt and PtRu electrodes, the onset of significant H_2 oxidation currents coincides with the *ignition potential* observed in 2% CO/Ar mixtures at ~0.75 and ~0.50 V, respectively, and occurs therefore upon the stripping of adsorbed CO which effectively blocks H_2 oxidation. Upon CO stripping, the H_2 oxidation current densities closely approach the diffusion-limited current density in pure H_2 (indicated in Fig. 5b). On PtSn electrodes, the increase in H_2 oxidation currents is very gradual and follows the CO oxidation behavior in 2% CO in Ar.

At a current density of 0.5 mA/cm^2 (*i.e.*, the contribution from mass transfer resistances to the measured current density is less than 15%), the electrode potential on the PtSn alloy is ~0.12 V lower than on the PtRu alloy and ~0.32 V lower than on pure Pt. This activity enhancement of the PtSn electrode over PtRu and pure Pt for the oxidation of a mixture of 2% CO in H_2 is less than what was observed for pure CO, where the electrode potential at the PtSn surface is ~0.20 eV lower than on PtRu ($x_{Ru,s}$~0.5) and ~0.38 V lower than on pure Pt /15, 18/. The reason for the decrease of the activity enhancement of the PtSn electrode over PtRu and Pt electrodes with a decrease in the CO concentration, is the logical consequence of the positive reaction order with respect to solution phase CO on PtSn (*i.e.*, *decrease* in activity with decreasing CO concentration) *versus* the negative reaction order on PtRu and Pt (*i.e.*, *increase* in activity with decreasing CO concentration).

As the CO concentration in the CO/H_2 mixture is reduced even further (1000 ppm CO in H_2, Fig. 6), the activity enhancement (evaluated at 0.5 mA/cm^2) of the PtSn electrode over PtRu and pure Pt decreases to 0.08 and 0.28 V, respectively. Therefore, the superior CO oxidation activity of PtSn *versus* PtRu alloy surfaces is the more pronounced, the higher the CO concentration in the gas mixture, being the highest for pure CO. Even at these low CO concentrations, practically no oxidation currents below 0.2 V can be observed on either PtSn or Pt electrodes, indicating a densely packed CO monolayer which is responsible for the complete suppression of H_2 oxidation at potentials which are negative of the onset potential for CO oxidation. On PtRu alloy surfaces, however, substantial H_2 oxidation current densities are measured at steady-state between 0.05 and 0.2 V /15/, *i.e.*, prior to the onset of CO oxidation. This effect can only be explained by assuming that the CO equilibrium coverage on PtRu surfaces at 60°C decreases slightly with the CO concentration in the

electrolyte, thereby producing holes in the CO layer which provide access for H_2 adsorption and oxidation /15/. The number of holes increases with both increasing temperature and decreasing CO concentration, and it is most likely the effect of holes and not the stripping of adsorbed CO which is responsible for the reported CO-tolerance of ~100 ppm for PtRu electrodes in H_2-PEMFC's at 80°C /11/.

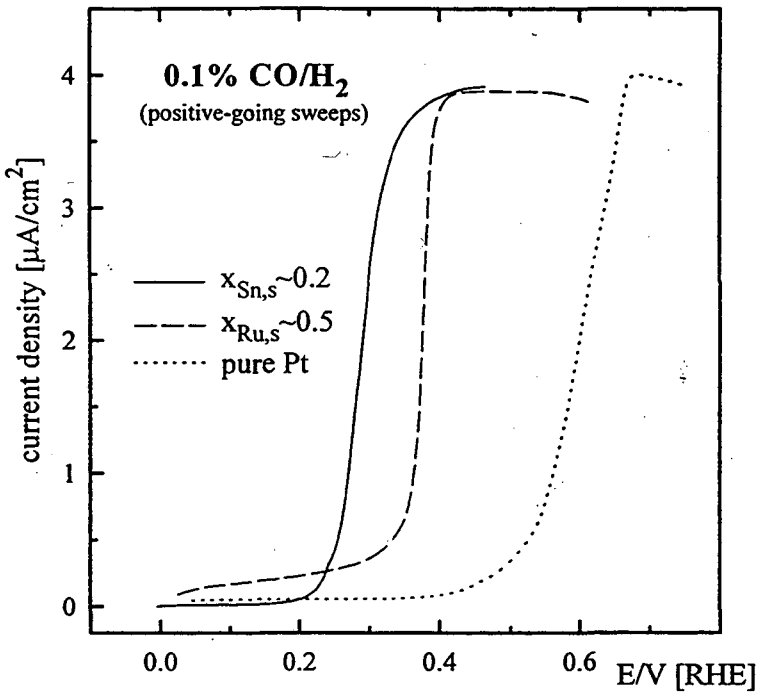

Fig. 6. Potentiodynamic oxidation (positive-going sweeps at 1 mV/s) of 0.1% CO/H_2 on UHV-prepared surfaces (sputtered with 0.5 keV Ar^+): (———) $Pt_3Sn(110)$ electrode with $x_{Sn,s}$~0.2; (— — —) PtRu(polycryst.) electrode with $x_{Ru,s}$~0.5; (· · · · · ·) polycrystalline Pt-disk electrode. Experiments were conducted at 60°C in 0.5 M H_2SO_4 at 2500 rpm. Prior to recording the potential scan, the electrodes were held at 0.05 V for 5 min. at 2500 rpm.

4. Conclusions

The CO oxidation activity of PtSn electrodes under fuel cell relevant conditions (~60°C and continuous supply of the reactant) is significantly higher than of PtRu and Pt electrodes. For pure CO, the catalytic shift of the PtSn alloy with a surface composition of $x_{Sn,s}$~0.2 amounts to ~0.2 and ~0.38 V if compared to PtRu ($x_{Ru,s}$~0.5) and Pt, respectively. The activity enhancement of PtSn electrodes decreases as the CO concentration is decreased, so that the activity enhancement for the oxidation of CO/H_2 gas mixtures is somewhat smaller, namely ~0.08 V *versus* PtRu and ~0.28 V *versus* Pt in a gas mixture of 1000 ppm CO in H_2. This effect is explained by the difference in reaction order for CO oxidation with respect to CO concentration: the positive reaction order on PtSn electrodes produces a *decrease* in the CO oxidation activity with *decreasing* CO concentration, while the negative reaction order on PtRu and Pt electrodes leads to an *increase* in CO oxidation

activity as the CO concentration *decreases*. On the basis of a Langmuir-Hinshelwood reaction mechanism, the negative reaction order with respect to solution phase CO on PtRu and Pt electrodes is rationalized by a competition between OH_{ads} nucleation and CO adsorption on Ru surface atoms. This competition does not occur on the OH_{ads} nucleating Sn surface atoms of PtSn electrodes owing to the inability of Sn to adsorb CO, thereby leading to a positive reaction order. CO and H_2 electrooxidation on PtSn electrodes occurs with high rates at a largely CO covered surface, in contrast to the oxidation mechanism on PtRu and Pt electrodes, where the onset of CO oxidation coincides with the complete oxidative stripping of adsorbed CO.

5. Acknowledgments

We are greatly indebted to Lee Johnson and Frank Zucca for their invaluable help in preparing the electrode samples and building innumerous experimental gadgets, without which we would not have been able to carry out this research. Also, we would like to acknowledge the work of our summer student Andrew Martin who wrote the programs for the digital data acquisition. This work was supported by the Assistant Secretary for Conservation and Renewable Energy, Office of Transportation Technologies, Electric and Hybrid Propulsion Division of the U.S. Department of Energy under Contract No. DE-AC03-76SF00098.

6. References

/1/ J. Haggin, *Chemical & Engineering News* **July 24**, 8 (1995)

/2/ M.S. Wilson, J.A. Valerio, S. Gottesfeld, *Electrochim. Acta* **40**, 355 (1995)

/3/ V.M. Schmidt, P. Bröckerhoff, B. Höhlein, R. Menzer, U. Stimming, *J. Power Sources* **49**, 299 (1994)

/4/ Daimler-Benz AG, "NECAR II - Driving without Emissions", Daimler-Benz AG, Stuttgart (Germany), 1996

/5/ R. Kumar, S. Ahmed, Proceedings of the First International Symposium on New Materials for Fuel Cell Systems, O. Savadogo, P.R. Roberge, T.N. Veziroglu (Eds.), École Polytechnique de Montréal: Montréal, pp. 224-238 (1995)

/6/ R.A. Lemons, *J. Power Sources* **29**, 251 (1990)

/7/ M. Watanabe, H. Uchida, H. Igarashi, M. Suzuki, *Chem. Lett.* **January Issue**, 21 (1995)

/8/ M. Kahlich, H.A. Gasteiger, R.J. Behm, *J. Catal.* in press.

/9/ M. Haruta, A. Ueda, S. Tsubota, R.M. Torres Sanchez, *Catalysis Today* **29**, 443 (1996)

/10/ M. Kahlich, M.M. Schubert, M. Hüttner, M. Noeske, H.A. Gasteiger, R.J. Behm, submitted to "Proceedings of the Second International Symposium on New Materials for Fuel Cell Systems", École Polytechnique de Montréal: Montréal, Juli 1997

/11/ H.-F. Oetjen, V.M. Schmidt, U. Stimming, F. Trila, *J. Electrochem. Soc.* **143**, 3838 (1996)

/12/ E.Ticanelli, J.G. Beery, M.T. Paffett, S. Gottesfeld, *J. Electroanal. Chem.* **258**, 61 (1989)

/13/ H.A. Gasteiger, N.M. Marković, P.N. Ross (Jr.), E.J. Cairns, *J. Phys. Chem.* **98**, 617 (1994)

/14/ H.A. Gasteiger, N.M. Marković, P.N. Ross (Jr.), *J. Phys. Chem.* **99**, 8290 (1995)

/15/ H.A. Gasteiger, N.M. Marković, P.N. Ross (Jr.), *J. Phys. Chem.* **99**, 16757 (1995)

/16/ S. Motoo, M. Watanabe, *J. Electroanal. Chem.* **69**, 429 (1976)

/17/ H.A. Gasteiger, N.M. Marković, P.N. Ross (Jr.), *J. Phys. Chem.* **99**, 8945 (1995)

/18/ H.A. Gasteiger, N.M. Marković, P.N. Ross (Jr.), "Structural Effects in Electrocatalysis: Electrooxidation of Carbon Monoxide on Pt3Sn Single-Crystal Alloy Surfaces", *Catal. Lett.* **36**, 1 (1996)

/19/ A. Boulahouache, G. Kons, H.-G. Lintz, P. Schulz, *Appl. Catal. A* **91**, 115 (1992)

/20/ M.T. Paffett, S.C. Gebhard, R.G. Windham, B.E. Koel, *J. Phys. Chem.* **94**, 6831 (1990)

/21/ A. Haner, P.N. Ross (Jr.), U. Bardi, A. Atrei, *J. Vac. Sci. Technol. A* **10**, 2718 (1992)

/22/ N.M. Marković, H.A. Gasteiger, P.N. Ross (Jr.), *J. Phys.Chem.* **99**, 3411 (1995)

/23/ A.M. Castro Luna, M.C. Giordano, A.J. Arvia, *Electrochim. Acta* **259**, 173 (1989).

/24/ T. Frelink, W. Visscher, J.A.R. van Veen, *Electrochim. Acta* **39**, 1871 (1994).

/25/ Y. Morimoto, E.B. Yeager, Extended Abstracts, ECS Spring Meeting in Reno (Nevada), 727 (1995).

/26/ M.J. Weaver, S.-C- Chang, L.-W.H. Leung, X. Jiang, M. Rubel, M. Szklarczyk, D. Zurawski, A. Wieckowski, *J. Electroanal. Chem.* **327**, 247 (1992).

/27/ K. Wang, H.A. Gasteiger, N.M. Marković, P.N. Ross (Jr.), *Electrochim. Acta* **41**, 2587 (1996).

/28/ A.J. Bard, L.R. Faulkner, Electrochemical Methods, John Wiley and Sons: New York, p. 283 (1980).

/29/ T. Engel, G. Ertl, G., *Adv. Catal.* **28**, 1 (1979).

Ernest Orlando Lawrence Berkeley National Laboratory
One Cyclotron Road | Berkeley, California 94720

Prepared for the U.S. Department of Energy under Contract No. DE-AC03-76SF00098